Appl. Phys. A 79, 677–680 (2004)
DOI: 10.1007/s00339-003-2232-3

Applied Physics A
Materials Science & Processing

D.W. KIM[1]
K.S. HONG[1,✉]
C.H. KIM[2]
K. CHAR[3]

Crystallographic orientation dependence of the dielectric constant in polymorphic $BaNb_2O_6$ thin films deposited by laser ablation

[1] School of Materials Science and Engineering, College of Engineering, Seoul National University, Seoul 151-742, Korea
[2] Department of Materials Science and Engineering, Case Western Reserve University, Cleveland, Ohio 44106-7204, USA
[3] School of Physics and Center for Strongly Correlated Materials Research, Seoul National University, Seoul 151-742, Korea

Received: 15 April 2003/Accepted: 20 May 2003
Published online: 16 July 2003 • **© Springer-Verlag 2003**

ABSTRACT Well-crystallized barium metaniobate ($BaNb_2O_6$) thin films were fabricated on fused quartz substrates by pulsed laser deposition. The influence of substrate temperature and oxygen pressure on the crystal structure and preferred orientation were studied to understand the growth mechanism of $BaNb_2O_6$ thin films. The films formed at 600 °C at an oxygen pressure of 100 mTorr exhibited predominantly the orthorhombic (040) orientation, and turned to the orthorhombic (230) orientation at 800 °C. It was found that (220)-oriented hexagonal thin films were formed at 600 °C at an oxygen pressure less than 50 mTorr. The dielectric constant of the $BaNb_2O_6$ thin films was measured by scanning microwave microscopy (SMM). Preferentially (230)-oriented orthorhombic and (220)-oriented hexagonal $BaNb_2O_6$ thin films were shown to have significantly enhanced dielectric constants of 47.8 and 56.7, respectively. This could be attributed to the dependence of the dielectric constant on crystallographic orientation.

PACS 77.55.+f; 77.84.Dy

1 Introduction

Ferroelectric $Sr_xBa_{1-x}Nb_2O_6$ $(0.25 \leq x \leq 0.75)$ with the tetragonal tungsten bronze structure has attracted a great deal of attention recently, and is currently being investigated as a potential material for pyroelectric, electro-optic, and photorefractive devices [1, 2]. However, little attention has been given to $BaNb_2O_6$ bulk ceramics and their thin films. Although crystallographic data for $BaNb_2O_6$ is not readily available, much research has been focused on the phase transitions of this material [3, 4]. Recently, it was reported that the hexagonal phase of $BaNb_2O_6$ transforms above 1200 °C to the orthorhombic structure [5]. In our previous work, we investigated the microwave dielectric properties of $BaNb_2O_6$ polymorphs [6, 7]. The dielectric properties of each phase are significantly different. An interesting feature of $BaNb_2O_6$ polymorphs is that orthorhombic $BaNb_2O_6$ has low loss ($\varepsilon_r = 30$, $Q \times f = 43\,000$ GHz, $Q \approx 1/\tan\delta$) and hexagonal $BaNb_2O_6$ has a higher dielectric constant of $42 (Q \times f = 4000$ GHz).

✉ Fax: +822-886/4156, E-mail: kshongss@plaza.snu.ac.kr

Microelectronics research is in large part driven by the demand for smaller components with enhanced performance. For capacitive components, which form the basis of many memory devices, the dielectric constant limits the degree of miniaturization – a limit that is now being approached for the materials currently in use. So far, modification of the dielectric constant has been achieved by using barium strontium titanate and tantalum oxide, and so on. Work on the preparation and performance of microwave dielectric thin films, such as the Zr-Sn-Ti-O system and $Ba_2Ti_9O_{20}$, has been published recently, because of their low loss and temperature stability [8–10]. The emphasis of the current work is to examine the preferential orientation of polymorphic $BaNb_2O_6$ thin films deposited by laser ablation. Here, we also report the enhanced dielectric constant of $BaNb_2O_6$ thin films using scanning microwave microscopy (SMM) for the accurate measurement of the dielectric constant in the microwave frequency region.

2 Experimental procedure

$BaNb_2O_6$ thin films of 3000-Å thickness were deposited on fused quartz substrates using a 248 nm KrF excimer laser (Lambda Physik Compex 205). $BaNb_2O_6$ targets were fabricated using the conventional mixed-oxide method. The laser energy density on the target surface was set to be 4 J/cm^2. After deposition, the films were cooled to room temperature at a rate of 5 °C/min. The structure of the thin films was investigated by X-ray diffraction and Raman spectroscopy. The surface morphology was investigated using an atomic force microscope (AFM). The dielectric constant was measured using a scanning microwave microscope (SMM) that was capable of investigating the local properties of materials in the rf/microwave frequency region. The dielectric constant could be obtained by measuring the shift of the resonant frequency of a quarter-wavelength coaxial resonator in the near-field regime. In this experiment, we used a 5-cm-long probe resonator with a resonant frequency near 1.5 GHz. The detailed schematic diagram has been reported elsewhere [11]. For the quantitative analysis of the dielectric constant of the thin films, the shift of the resonant frequency of the probe was calculated for the thin films on fused quartz ($\varepsilon_r = 3.5$) substrate, and the fitting functions were derived as functions of the tip-sample distance [12].

3 Results and discussion

Figure 1 shows the relative dielectric constant and the dielectric loss tangent ($\tan\delta$) of the $BaNb_2O_6$ thin films deposited on $Pt(111)/TiO_2/SiO_2/Si$ substrates using rf-magnetron sputtering, measured in the frequency range of 1 to 10 MHz. Polycrystalline films with orthorhombic structure were obtained after annealing at 700 °C for 3 hours. The experimental details are not described here. ε_r and $\tan\delta$ were about 30.2 and 0.004, respectively. The $BaNb_2O_6$ thin films exhibited good dielectric properties consistent with the values measured for the bulk ceramics. The XRD patterns of the $BaNb_2O_6$ thin films are presented as a function of substrate temperature and oxygen pressure in Fig. 2. It can be seen that substrate temperature and oxygen pressure were found to be important for controlling the crystallographic orientation. It can be seen in Fig. 2a that the threshold for crystallization at an oxygen pressure of 100 mTorr was at a substrate temperature of 600 °C. Preferentially (400)-oriented orthorhombic $BaNb_2O_6$ thin films were obtained at 650 °C. Further increasing the substrate temperature caused the intensity of the (230) peak to increase, and a change in orientation was observed at 800 °C. The change of the films was confirmed by the measurement of the surface morphology by AFM, as shown in Fig. 3. In the case of (400)-oriented films, columnar grains growing perpendicular to the surface of the film were observed. For the (230)-oriented films, the growth occurred with the basal planes parallel to the substrate surface. This behavior is also coincident with the change of the preferential orientation of the deposited $BaNb_2O_6$ films with orthorhombic structure. As the deposition temperature was increased, atomic rearrangement took place due to the increase of adatom mobility, leading to the change of orientation. Keeping the substrate temperature at 600 °C, an oxygen pressure below 100 mTorr was required for the crystallization of the $BaNb_2O_6$ films. With a decrease of the oxygen pressure from 100 to 50 mTorr, the (400)-oriented orthorhombic $BaNb_2O_6$ films were transformed completely to highly (220)-oriented hexagonal $BaNb_2O_6$ films. Figure 4 shows the unpolarized Raman spectra of the highly oriented $BaNb_2O_6$ films. The spectra of the $BaNb_2O_6$ thin films with hexagonal and orthorhombic structures indicated

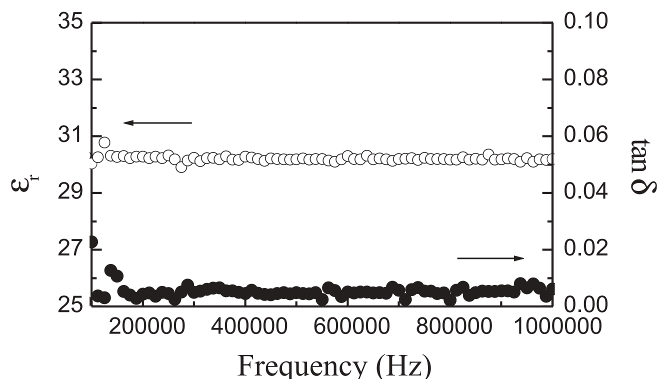

FIGURE 1 The typical frequency dependence of the relative dielectric constant (ε_r) and dielectric loss tangent ($\tan\delta$) of the orthorhombic $BaNb_2O_6$ thin film at 1–10 MHz

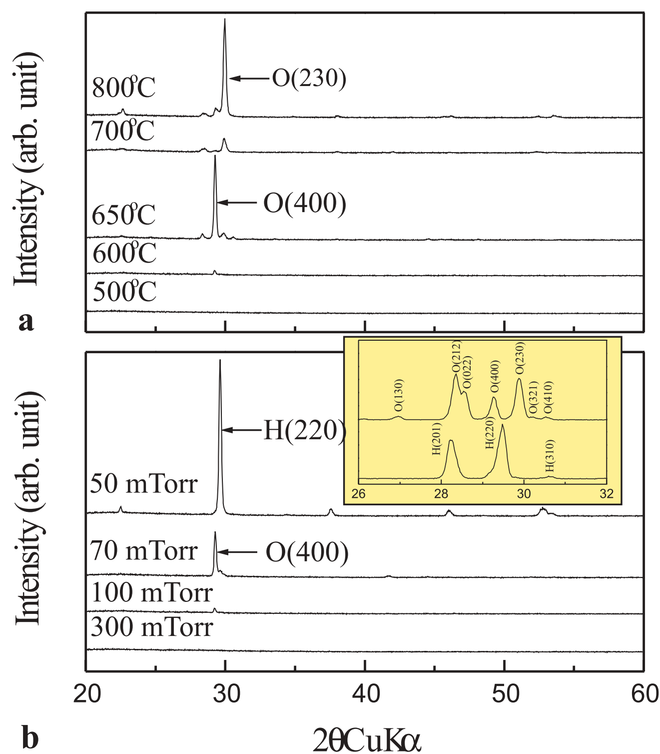

FIGURE 2 XRD patterns of $BaNb_2O_6$ thin films on fused quartz deposited at **a** different substrate temperatures at an oxygen pressure of 100 mTorr and **b** 600 °C at different oxygen pressures (H: hexagonal; O: orthorhombic; the *inset* shows a magnified view of XRD patterns for bulk $BaNb_2O_6$ ceramics)

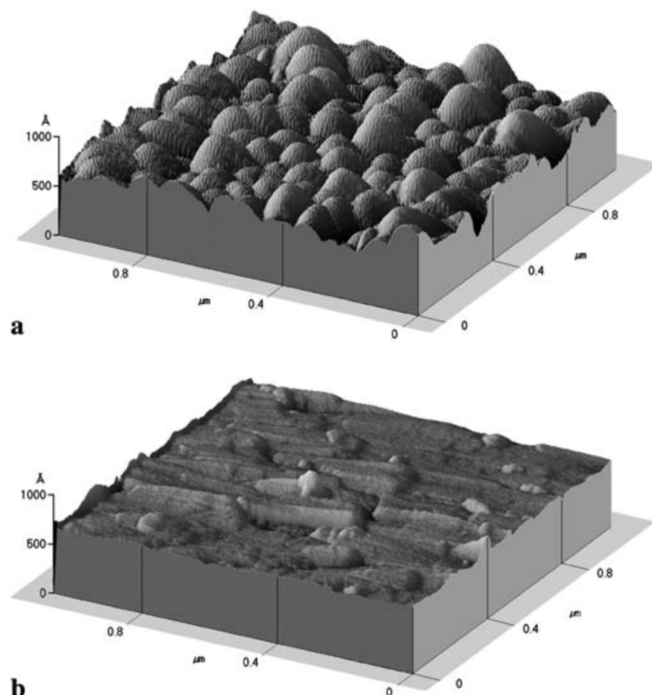

FIGURE 3 Three-dimensional AFM images of $BaNb_2O_6$ thin films at **a** 650 °C and **b** 800 °C at an oxygen pressure of 100 mTorr

good coincidence with the structures of $BaNb_2O_6$ bulk samples (the inset of Fig. 4). The Raman spectra of $BaNb_2O_6$ were originally reported by Repelin et al. [13]. They characterized the spectra by NbO_6 octahedra with orthorhombic structure, but the spectra given are similar to the hex-

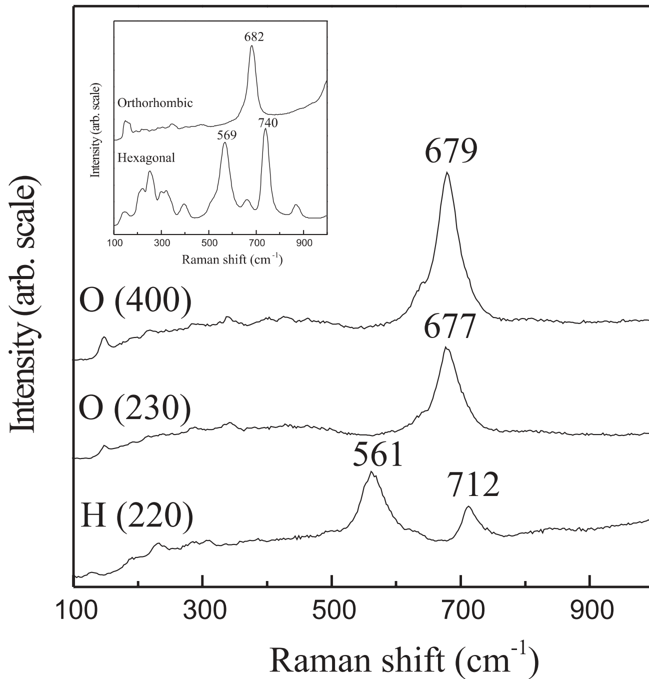

FIGURE 4 Raman spectra of preferentially oriented $BaNb_2O_6$ thin films (H: hexagonal; O: orthorhombic; the *inset* shows Raman spectra for bulk $BaNb_2O_6$ ceramics)

agonal spectra of our study. Our results are supported by the spectra of sol–gel-derived $BaNb_2O_6$ powders with hexagonal structure, given by Ho et al. [14]. Our study also confirms the polymorphs of $BaNb_2O_6$ from the Raman modes.

It has been reported that the hexagonal phase of $BaNb_2O_6$ can be considered a low-temperature phase [5]. At 600 °C at an oxygen pressure below 50 mTorr, we could get hexagonal thin films, which may be due to the depletion of oxygen in the films. The same trend has been observed in MoO_3 thin films, which have a structure related to the three-dimensional ReO_3 structure [15]. It has been reported that the $BaNb_2O_6$ structure is also produced from an ReO_3-like framework [16]. The inset in Fig. 2 is an enlargement of the main peak region in XRD powder diffraction profiles of $BaNb_2O_6$. It is evident that the diffraction lines observed for the orthorhombic structure can be derived by splitting the diffraction lines found in the hexagonal form [3]. The orthorhombic structure may be described using a hexagonal primitive cell. The a_o dimension in the hexagonal and orthorhombic structures are nearly identical, and the b_o and c_o axial lengths in the orthorhombic structure are approximately $\sqrt{3}/2$ and 2 times a_o and c_o in the hexagonal structure [3, 17]. In both the polymorphic structures, unit cell dimensions are closely related. The hexagonal-to-orthorhombic phase transition can be classified as topotaxy with preservation of the axes of symmetry [6]. Thus, orthorhombic (400) and (230) reflections have the same nature derived from the hexagonal (220) reflection. Here, the preferentially (220)-oriented hexagonal thin film can be explained based on Wulff's theorem. As reported for (Zr, Sn)TiO_4 thin films [18], the hexagonal (220) plane is stable, with a lower surface energy than the hexagonal (201) plane.

Near-field scanning microwave microscopy detects a combination of both the in-plane and out-of plane components of the dielectric matrix and is able to map local variations of dielectric properties. We have measured the quantitative dielectric constant of highly oriented thin films quite accurately, changing the tip–sample distance at each point using scanning microwave microscopy (SMM). The relationship between the frequency shift and the dielectric constant (ε) is expressed as

$$-\frac{\Delta f}{A f_\mathrm{r}} = \left(\frac{\varepsilon+1}{\varepsilon-1}\right) \ln\left(\frac{2}{\varepsilon+1}\right) + 1\,, \tag{1}$$

where f_r, ε, and A are the resonant frequency of the probe resonator, the dielectric constant, and an unknown parameter depending on the probe resonator, respectively [19]. We were able to determine the unknown parameter A from the resonant frequency in air and the dielectric constant of the substrate (3.75) using (1). Figure 5 shows the simulation for the contact mode of $-\Delta f/A f_\mathrm{r}$ for the thin film on fused quartz, as a function of the relative dielectric constant (ε_r) of the film [12]. The measured ε_r of all of the aforementioned $BaNb_2O_6$ thin films at room temperature is shown in Fig. 6. Although the polycrystalline $BaNb_2O_6$ film had a similar ε_r (30) to the bulk ceramic when measured by the LCR meter at 1–10 MHz, as shown in Fig. 1, remarkably different ε_r were measured in highly oriented films using SMM. The ε_r of the (400)-oriented orthorhombic film was 33.1, while the (230)-oriented orthorhombic and (220)-oriented hexagonal films exhibited enhanced ε_r of 47.8 and 56.7, respectively. In bulk ceramics, hexagonal $BaNb_2O_6$ has a higher dielectric constant (42) than orthorhombic $BaNb_2O_6$ (30). Thus, hexagonal thin films are expected to show higher dielectric constants than orthorhombic films, but no structure–dielectric property correlation for $BaNb_2O_6$ has been established to explain the observed dielectric anisotropy. Several investigations have been made of the

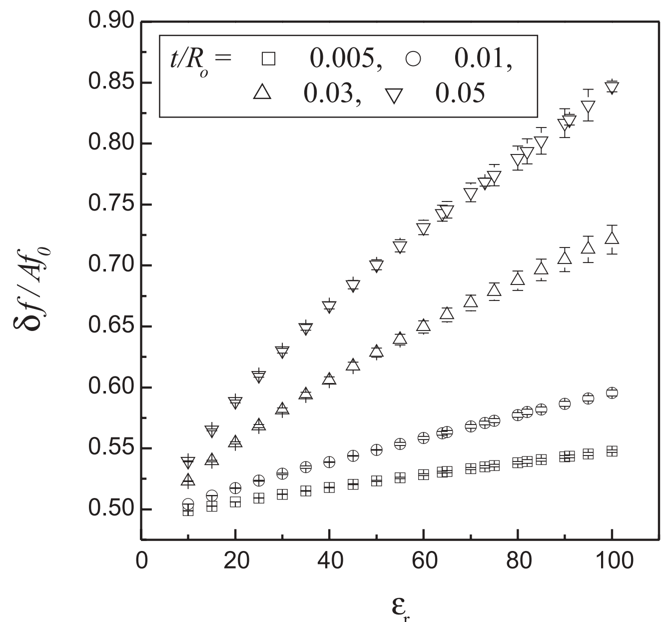

FIGURE 5 Simulated resonant frequency shift ($-\Delta f/A f_\mathrm{r}$) as a function of the relative dielectric constant (ε_r) for thin films on fused quartz (t: thickness of the thin film; R_o: tip radius)

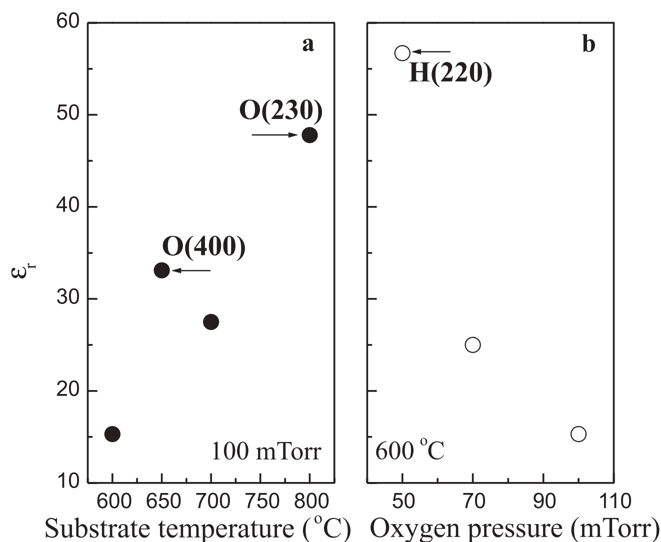

FIGURE 6 ε_r of $BaNb_2O_6$ thin films at 1.5 GHz as a function of **a** substrate temperature and **b** oxygen pressure (H: hexagonal; O: orthorhombic)

crystallographic orientation dependence of dielectric properties [20–22]. We think that the highly crystallized structure of the orthorhombic (230) and hexagonal (220) orientations is most probably the main cause of the high dielectric constant of $BaNb_2O_6$ thin films. Joshi et al. have also suggested that the high dielectric constant in Ta_2O_5 thin films is due to strong *a*-axis orientation, based on the calculated value of the dielectric polarizability in the Clausius–Mossotti equation [23].

4 Conclusions

In summary, this work demonstrates dielectric anisotropy in polymorphic $BaNb_2O_6$ thin films whose preferential orientations are sensitive to preparation conditions. We have elaborated on the structure and orientation of $BaNb_2O_6$ thin films using AFM images and Raman shifts. Bulk $BaNb_2O_6$ ceramics have dielectric constants of 30–42, but preferentially (230)-oriented orthorhombic and (220)-oriented hexagonal $BaNb_2O_6$ thin films show significantly enhanced dielectric constants of 47.8 and 56.7, respectively, in the microwave frequency range. Although detailed tests of the performance of $BaNb_2O_6$ were not carried out, the study of the processing and dielectric properties of this new material in thin film form may be of significant interest for high-frequency applications, such as dynamic random access memory (DRAM) and monolithic microwave integrated circuits (MMIC).

ACKNOWLEDGEMENTS The authors acknowledge support of this work through the Research Institute of Advanced Materials, Seoul National University.

REFERENCES

1 P.V. Lenzo, E.G. Spencer, A.A. Ballman: Appl. Phys. Lett. **11**, 23 (1967)
2 R.R. Neurgaonkar, W.K. Cory: J. Opt. Soc. Am. B: Opt. Phys. **3**, 274 (1986)
3 M.H. Francombe: Acta Cryst. **13**, 131 (1960)
4 L.M. Kovba, L.N. Lykova, Z.Y. Kulikova, P.P. Leshchenko, I.P. Zapasskaya: Moscow Univ. Chem. Bull. **33**, 69 (1978)
5 O. Yamaguchi, K. Matsui, K. Shimizu: J. Am. Ceram. Soc. **68**, C173 (1985)
6 D.W. Kim, H.B. Hong, K.S. Hong, C.K. Kim, D.J. Kim: Jpn. J. Appl. Phys. **41**, 6045 (2002)
7 D.W. Kim, J.R. Kim, S.H. Yoon, K.S. Hong, C.K. Kim: J. Am. Ceram. Soc. **85**, 2759 (2002)
8 F.J. Wu, T.Y. Tseng: J. Am. Ceram. Soc. **81**, 439 (1998)
9 R.B. Van Dover, L.F. Schneemeyer, R.M. Fleming: Nature **392**, 162 (1998)
10 H.M. O'Bryan, R.K. Watts, S. Hou, Z.X. Ma: Integr. Ferroelectr. **15**, 155 (1997)
11 S. Hyun, A. Kim, J. Kwon, K. Char: Jpn. J. Appl. Phys. **40**, 6510 (2001)
12 J.H. Lee, S. Hyun, K. Char: Rev. Sci. Instrum. **72**, 1425 (2001)
13 Y. Repelin, E. Husson, H. Brusset: Spectrochim. Acta **35A**, 937 (1979)
14 M.M.T. Ho, C.L. Mak, K.H. Wong: J. Eur. Ceram. Soc. **19**, 1115 (1999)
15 O.M. Hussain, K. Srinivasa Rao, K.V. Madhuri, C.V. Ramana, B.S. Naidu, S. Pai, J. John, R. Pinto: Appl. Phys. A **75**, 417 (2002)
16 B.G. Hyde, S. Anderson: *Inorganic Crystal Structures* (Wiley, New York 1989)
17 R.S. Roth, J.L. Waring: J. Res. Natl. Bur. Stand. **65**, 337 (1961)
18 O. Nakagawara, Y. Toyota, M. Kobayashi, Y. Yoshino, Y. Katayama, H. Tabata, T. Kawai: J. Appl. Phys. **80**, 388 (1996)
19 C. Gao, X.D. Xiang: Rev. Sci. Instrum. **69**, 3846 (1998)
20 J.J. Araiza, M. Cardenas, C. Falcony, V.H. Mendez-Garcia, M. Lopez, G. Contreras-Puente: J. Vac. Sci. Technol. A **16**, 3305 (1998)
21 J. Lin, N. Masaaki, A. Tsukune, M. Yamada: Appl. Phys. Lett. **74**, 2370 (1999)
22 T. Sakai, T. Watanabe, Y. Cho, K. Matsuura, H. Funakubo: Jpn. J. Appl. Phys. **40**, 6481 (2001)
23 P.C. Joshi, M.W. Cole: J. Appl. Phys. **86**, 871 (1999)